Tsunami Hydrodynamic Force on Various Bridge Sections

H. Nakao
Public Works Research Institute, Japan

K. Nozaka, K. Izuno & H. Kobayashi
Ritsumeikan University, Japan

15 WCEE
LISBOA 2012

SUMMARY:
This paper discusses tsunami induced hydrodynamic forces applied to various bridge sections through hydraulic experiments. The hydraulic experiments were conducted using bridge models with rectangular, trapezoidal, inverted trapezoidal, hexagonal, and mixed rectangular/semicircular (modified rectangular) cross-sectional geometries. During the experiments, the flow pattern around the models and the tsunami hydrodynamic forces were observed. The results showed that the trapezoidal, hexagonal, and modified rectangular section models were subjected to less horizontal hydrodynamic force than the rectangular section model. Further, it was shown that the trapezoidal and modified rectangular models were subjected to low lift forces, and that the tri-component force coefficients of all tested models were nearly constant regardless of the inundation depth of the wave. Additionally, the effect of countermeasure work performed on a plate girder bridge model was discussed. It was determined that even though the horizontal force could not be reduced significantly, vertical lift force could be reduced by installing baffle plates to the girders, thus reducing the risk that the bridge might be destroyed by a tsunami.

Keywords: Tsunami, Bridge, Hydraulic experiments, Retrofit, Baffle plates

1. INTRODUCTION

The tsunamis resulting from the Great East Japan Earthquake in March 2011 washed out numerous bridges. Those lost bridges resulted in serious disruption to the national lifeline system, which then delayed rescue activities and the progress of restoring the stricken towns and cities. To date, no Japanese bridges have been designed to withstand tsunami forces. Therefore, exploring ways to strengthen the bridges along tsunami-prone coastal areas is an important issue.

In the time since the 2004 earthquake struck off the coast of Sumatra, Indonesia, numerous experiments on tsunami bridge damage have been conducted in Japan, as shown in the references. Most of them, however, focused on determining if bridge bearings and/or connecting cables had the strength necessary to prevent the structures from being washing away by the wave. However, these are strictly mechanical measures.

Fluid dynamic related countermeasures, on the other hand, also have utility in bridge engineering, primarily in the field of wind engineering. By using fluid dynamic engineering measures, optimal cross-sectional geometries for reducing hydrodynamic forces could be determined.

Accordingly, this paper discusses the optimum cross-sectional geometry of bridge girders in terms of tsunami resistance through hydraulic experiments, after which a countermeasure for a plate girder bridge is explored.

2. HYDRAULIC EXPERIMENTS

2.1. Experimental Setup

The experimental flume shown in Figure 1 was used for our hydraulic experiments. The open channel flume is 200 mm wide and 4000 mm long, and was attached to a tank that was 600 mm wide and 2000 mm long. To simulate tsunami flow in the open channel, the water tank was filled with water while the open channel was left no water. The gate installed between the flume and the tank could be abruptly removed in order to generate a sudden wave similar in form to a tsunami.

The bridge model was set at 3000 mm downstream from the gate, and 40 mm above the flume bottom. A three-component load cell installed at the bridge model recorded horizontal, vertical and rotational tsunami force measurements at a sampling rate of 100 Hz. High frequency noise in the measured forces was removed by a 15 Hz low-pass filter. A water gauge installed 90 mm upstream from the bridge model measured the water level of the inundation flows. Flow pattern around the model was continuously photographed at a speed of 30 frames per second with a high-speed camera.

2.2 Bridge Models

Bridge models were fabricated in five cross-sectional types for use in our experiments: rectangle, trapezoid, inverted trapezoid, hexagon, and a rectangle with semicircles attached to both sides (modified rectangle). The models were created at a scale of 1:150, as shown in Figure 2. The positive axes of the measured forces are also displayed in the figure. The axis of the moment is located at the center of the model.

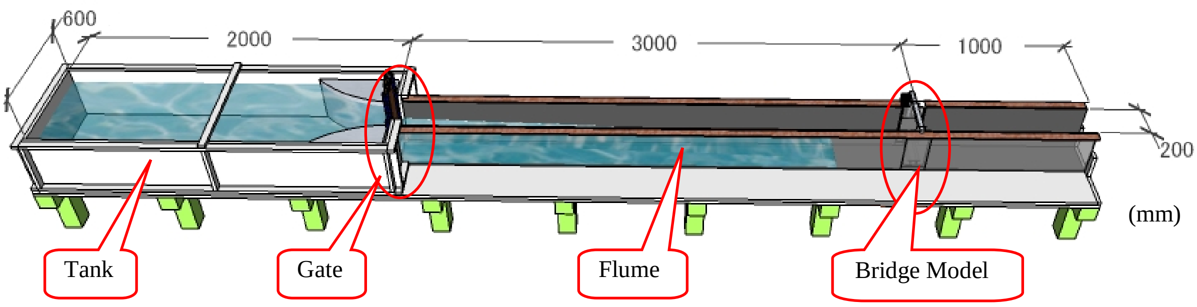

Figure 1. Schematic diagram of experimental flume

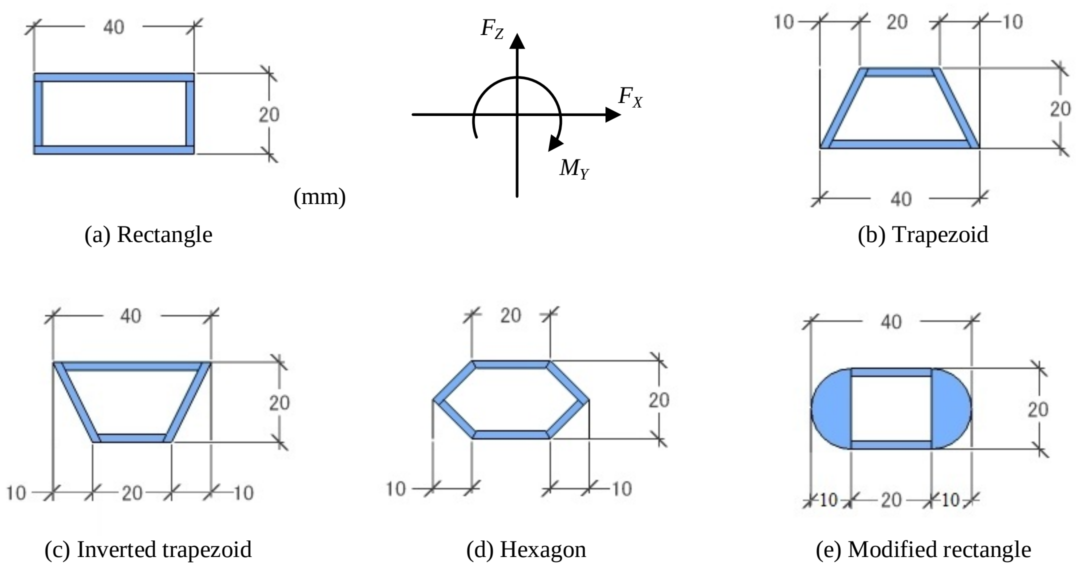

Figure 2. Bridge model cross-sectional geometries

3. TSUNAMI INDUCED FORCES

3.1 Flows Around Model

The initial height of the water in the tank was set to 300 mm. The water level at the upstream point of the bridge model by the water gauge was 78 mm, when no bridge model was set in place. Figure 3 shows photographs taken 0.2 seconds after the simulated tsunami reached the leading edge of the bridge model. Auxiliary lines are drawn to show the model and clarify the flow pattern of the initial tsunami actions.

As shown in Figure 3(a), the wave grew vertically when the rectangular cross-sectional model was used and wave overtopping was observed for the other model cross sections. The modified rectangular model experienced the smoothest flow, as shown in Figure 3(e).

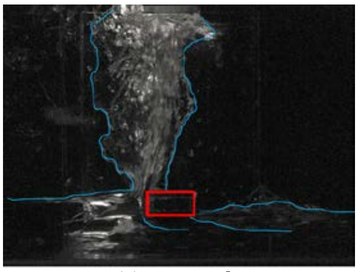
(a) Rectangle

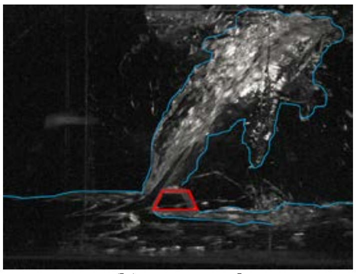
(b) Trapezoid

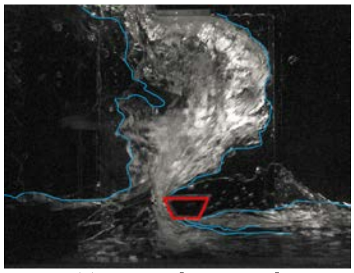
(c) Inverted trapezoid

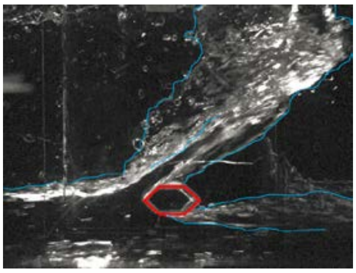
(d) Hexagon

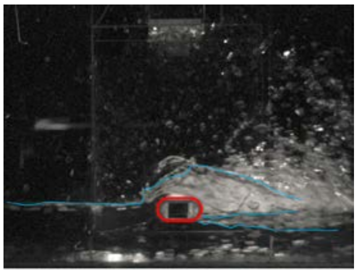
(e) Modified rectangle

Figure 3. Flow pattern at the initial impact

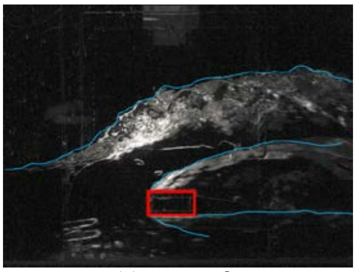
(a) Rectangle

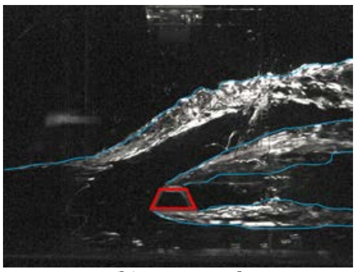
(b) Trapezoid

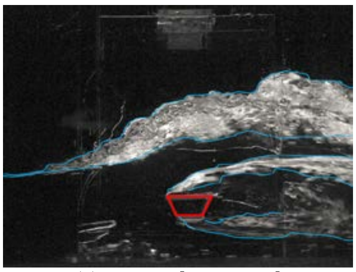
(c) Inverted trapezoid

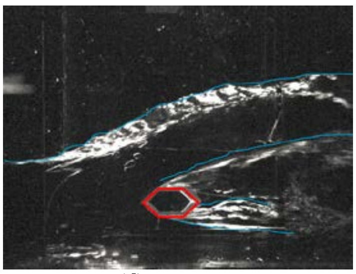
(d) Hexagon

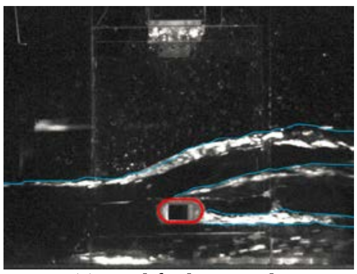
(e) Modified rectangle

Figure 4. Flow pattern at 1.0 seconds after tsunami impact

Figure 4 shows photographs taken 1.0 second after tsunami arrival at the models. These display the post tsunami impact conditions. Separated flows were observed in every case, but the modified rectangular model showed separated flow from only upper side of the girder, as shown in Figure 4(e).

These figures also show that the upstream water level increased as the bridge model disturbed the natural smooth flow of water. We found that the water level height at the upstream region of the model was lowest for the modified rectangular model. Furthermore, observations of Figures 3(e) and 4(e) showed the advantages of the modified rectangular cross-sectional design over the other section geometries in terms of tsunami resistance.

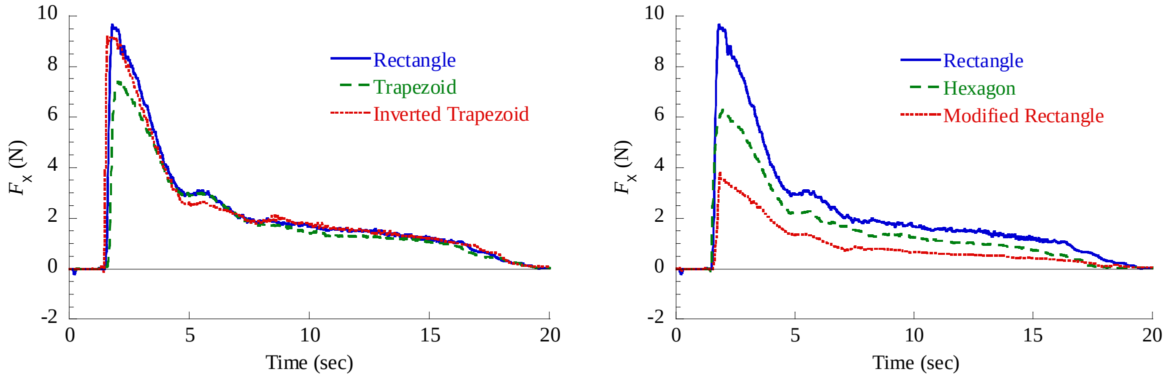

(a) Rectangle, trapezoid and Inverted trapezoid (b) Rectangle, hexagon, and modified rectangle

Figure 5. Drag (horizontal forces)

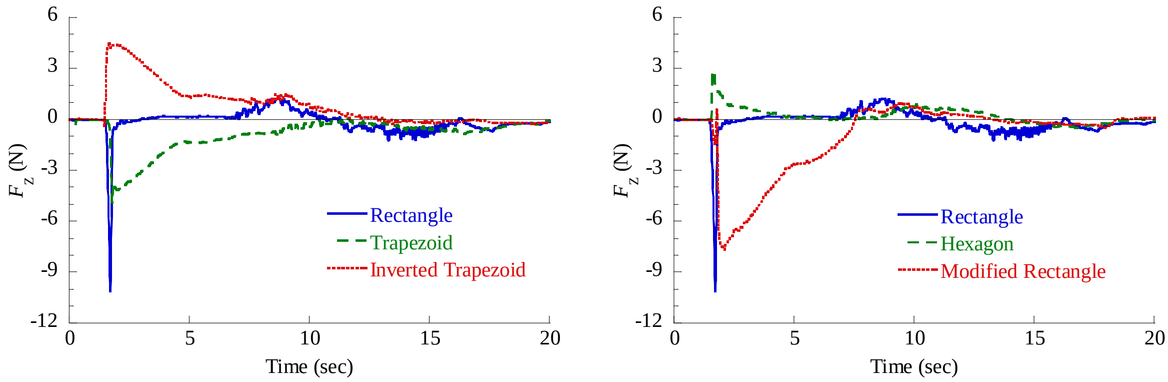

(a) Rectangle, trapezoid and Inverted trapezoid (b) Rectangle, hexagon, and modified rectangle

Figure 6. Lift (vertical forces)

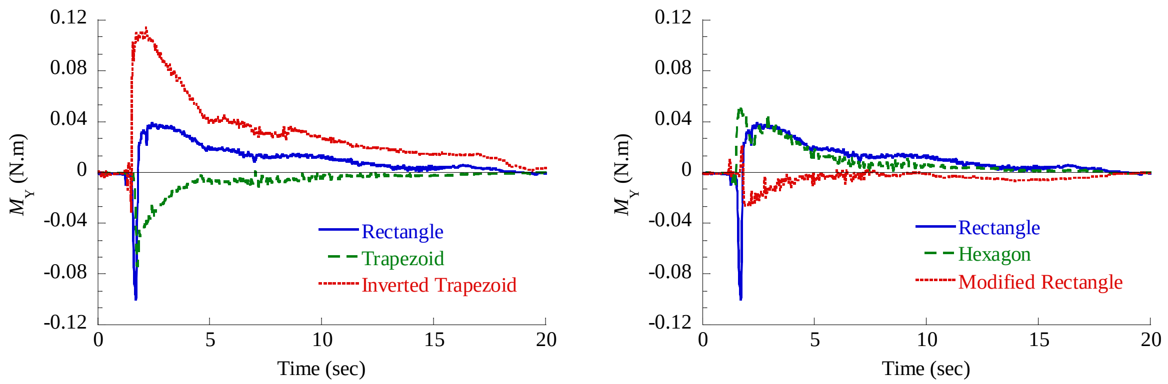

(a) Rectangle, trapezoid and Inverted trapezoid (b) Rectangle, hexagon, and modified rectangle

Figure 7. Moment

3.2 Forces Impacting Models

Figures 5-7 show the results of tsunami force impacts on the models as measured by the load cell. Figure 5 shows the drag (horizontal force) F_X, Figure 6 shows the lift (vertical force) F_Z, and Figure 7 shows the moment (rotational couple) M_Y, respectively.

Drag grew up rapidly after the tsunami reached the rectangular section model and took its highest value. The rectangular section model showed the highest drag, and the inverted trapezoidal model showed nearly the same drag, while the modified rectangular model showed the lowest (see Figure 5). The rectangular section also experienced an instant vertical downward force at the moment the wave arrived (see Figure 6). At this time, no separated flow affected on the upper side surface yet, and the separated flow from the lower leading edge of the model produced such downward force.

As shown in Figure 6, the trapezoidal and the modified rectangular models also encountered a vertical downward force, and the duration time was long. On the contrary, the inverted trapezoidal and hexagonal section models experienced only an uplift force.

From Figure 7, it can be seen that the rectangular section model first showed counterclockwise rotation because of the impulsive downward force produced near the leading edge of the model, after which it showed clockwise rotation because of the overtopping wave.

The inverted trapezoidal and hexagonal models showed clockwise rotation at all times, which indicates that a bridge constructed in a similar manner would be in severe danger of being washed away if struck by a tsunami. From Figures 6 and 7, the clockwise moment considered to be produced by the pressure on the inclined front side surface of the model. In contrast, the trapezoidal and modified rectangular models displayed counterclockwise rotation during the tsunami action.

4. MAXIMUM AND MINIMUM FORCE COEFFICIENTS

Tsunami forces can be expressed in terms of dimensionless quantities that include the drag coefficient (C_D), lift coefficient (C_L), and moment coefficient (C_M). These tri-component force coefficients are expressed as follows:

$$C_D = \frac{F_X}{0.5 \rho A U^2} \tag{1}$$

$$C_L = \frac{F_Z}{0.5 \rho A U^2} \tag{2}$$

$$C_M = \frac{M_Y}{0.5 \rho A B U^2} \tag{3}$$

in which ρ is the mass density of water (1000 kg/m^3), U is the flow speed of the tsunami, A is the projected frontal area of the model (4000 mm^2 in this experiment), and B is the width of the model cross-section (40 mm). The flow speed was calculated based on the distance between the gate and the model, divided by the travel time of the water between them. This speed varied between 1.5 and 2.0 m/s depending on the amount of water loaded in the tank.

The maximum and minimum forces on each model were picked from the measured forces shown in Figures 5-7. Then the force coefficients were calculated from Eqns. (1)-(3). Figure 8 shows the drag, lift, and moment coefficients derived from the experiments. The abscissa is the inundation ratio $h_{\max}/h_p$, which is defined as the maximum water height at the upstream point of the bridge model ($h_{\max}$), normalized by the clearance under the model h_p. The inundation ratio of 1.5 corresponds to the tsunami height at the upper surface of the bridge model.

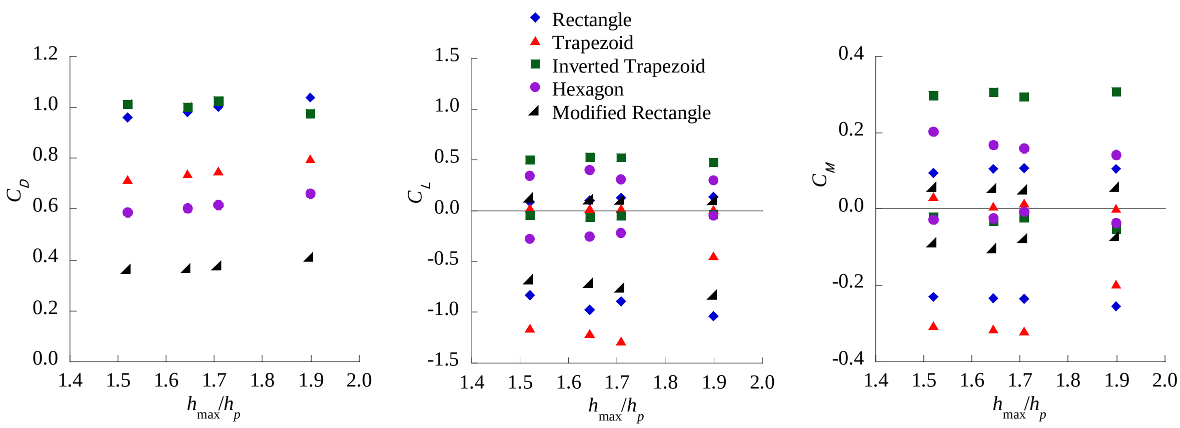

(a) Drag coefficients (b) Lift coefficients (c) Moment coefficients

Figure 8. Tri-component force coefficients

We found that the drag coefficient C_D was nearly constant regardless of the inundation ratio for each cross-sectional geometry tested. The rectangular model showed the highest values, approximately 1.0, while the modified rectangular model showed the lowest values, approximately 0.4.

The lift coefficients C_L were calculated both for upward and downward forces, as shown in Figure 8(b). The positive lift coefficients were almost constant, while the negative coefficients varied slightly depending on the inundation ratio. The inverted trapezoidal section showed the largest value (approximately 0.5.), while the trapezoidal section showed maximum negative coefficients (approximately -1.3).

The moment coefficients C_M were nearly constant for every cross-sectional geometry tested, and value variations tended to be similar to those recorded for the lift coefficients C_L.

Using the drag, lift and moment coefficients, the tsunami induced force could be calculated for each cross-sectional geometry studied, as long as the flow speed could be estimated. For example, the C_D for the rectangular section model can be set to 1.0 from Figure 8(a). Then, if the tsunami flow speed is estimated for the bridge location, the drag is calculated from Eqn. (1). As a result, new bridges can be designed, and existing bridges can be modified, to resist tsunami impact forces.

5. COUNTERMEASURE FOR PLATE GIRDER BRIDGE MODEL

In this section, we examine a tsunami countermeasure for existing bridges and discuss its efficacy. Figure 9(a) shows the assumed original cross section of a plate girder bridge model selected as an example. To retrofit this model, baffle plates were added to the outer sides of the model's girders, as shown in Figure 9(b).

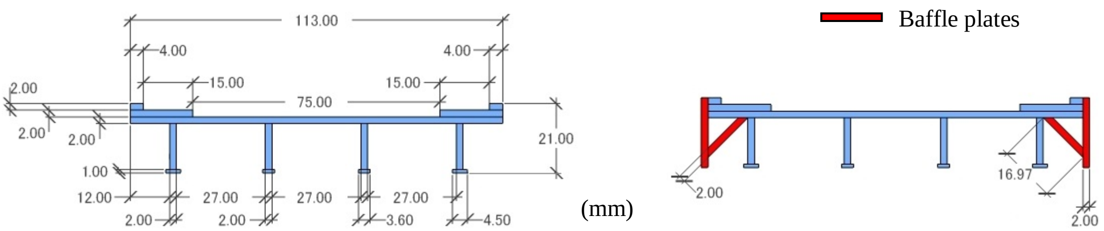

(a) Original model (b) Retrofitted model

Figure 9. Original and retrofitted plate girder bridge models

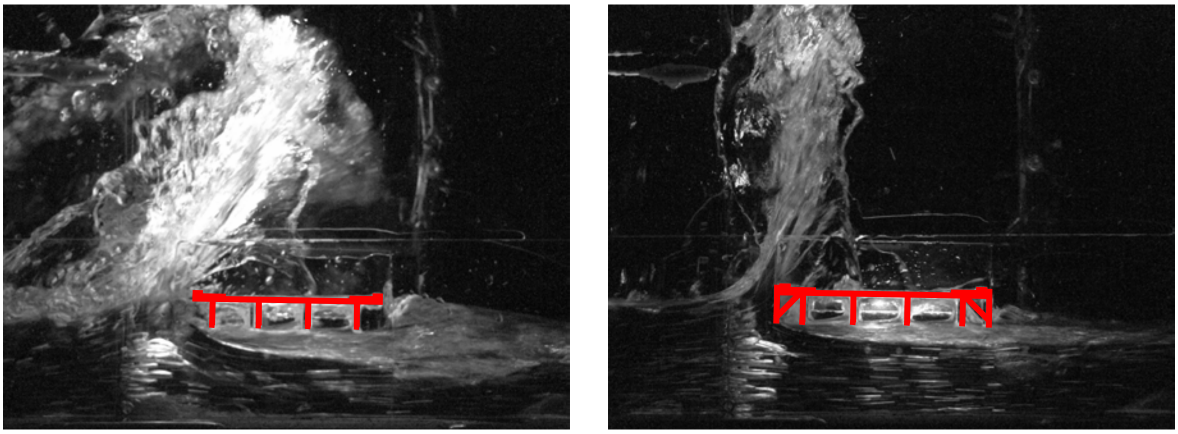

(a) Original model (b) Retrofitted model

Figure 10. Flow pattern around original and retrofitted models

Figure 10 shows the flow pattern of both models 0.2 seconds after the tsunami impact. Here it can be seen that the wave overtopped the original section as shown in Figure 10(a), and the overhanging section received the full forces of the dominant wave. In contrast, it can be seen that the wave grew vertically for the retrofitted model, as shown in Figure 10(b), much like the rectangular section shown in Figure 3(a).

Figure 11 shows the time histories of the tsunami induced forces for the original and the retrofitted models. Here, it can be seen that the drag for the retrofitted model was only 10% lower than that for the original model, as shown in Figure 11(a), thus indicating that the baffle plates did little to reduce horizontal tsunami forces.

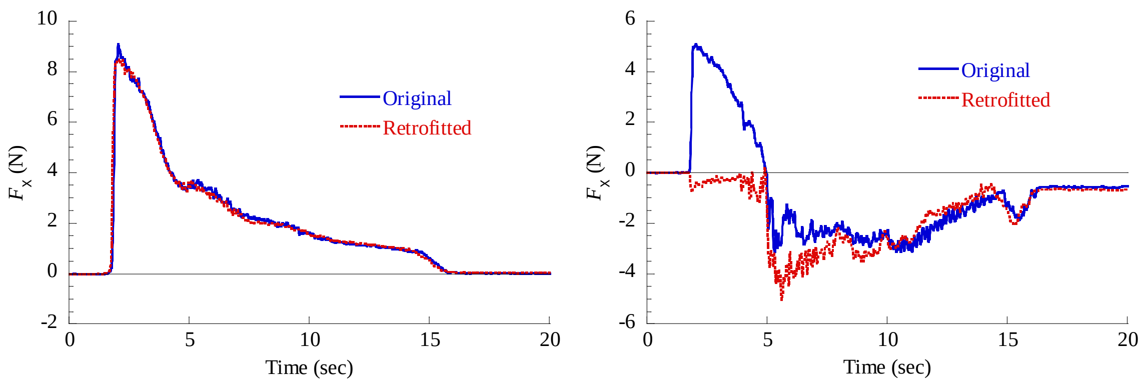

(a) Drag (b) Lift

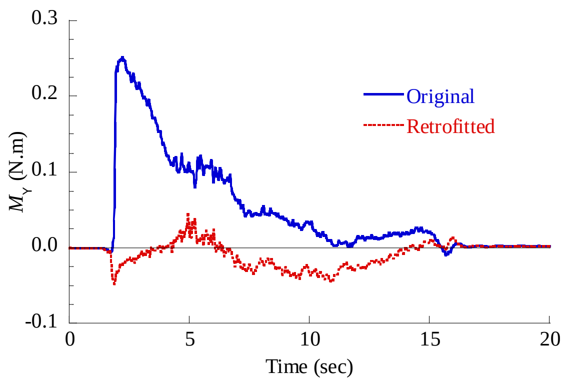

(c) Moment

Figure 11. Tsunami induced forces

On the other hand, the lift applied to the retrofitted model was reduced to almost zero, as shown in Figure 11(b). As the original model received uplift force due to the pressure acting on underneath of the overhanging section, it was determined that the baffle plates could counteract the weak points of the original section.

Even though the downward force imposed on the retrofitted model was more than 1.5 times that received by the original, bridges are generally more resistant to downward forces than they are to uplift forces, which tend to affect bridge bearings adversely.

Figure 11(c) shows the advantages of the retrofitted model. If a high clockwise moment was observed (like the original section), the bridge girders would be under high risk of being washed away. In contrast, the retrofitted model girders received high counterclockwise and low clockwise moments, which indicates that bridges so equipped would be at low risk of being washed away.

Furthermore, even though the drag could not be reduced significantly, lessening the upward lift and clockwise moment decreased the risk danger to the structure. Therefore, these results demonstrate the efficacy of adding baffle plates to plate girder bridges. In our future studies, we intend to investigate the use of curved baffle plates like Figure 2(e) for the modified rectangular model.

6. CONCLUSIONS

This paper discussed tsunami hydrodynamic force applied to various bridge section models through hydraulic experiments. The primary results obtained from this study were as follows:

1) Five model bridge cross sections (rectangle, trapezoid, inverted trapezoid, hexagon, and modified rectangle) were compared in hydraulic experiments. These experiments showed the simulated tsunami wave grew vertically for the rectangular cross-section, and the other model cross sections were subjected to wave overtopping after the initial tsunami impact. The modified rectangular model experienced the smoothest flow.

2) The rectangular section model received the highest drag, while the modified rectangular model showed the lowest. The rectangular, trapezoidal, and modified rectangular models experienced a vertical downward force. In contrast, the inverted trapezoidal and hexagonal section models encountered an upward lift.

3) Tri-component force (drag, lift, and moment) coefficients calculated from the experiments were relatively constant regardless of the inundation ratio for each model cross section.

4) A countermeasure for reducing tsunami force for a plate girder bridge was also examined. Baffle plates were attached to the outer sides of the girders. The results proved the efficacy of adding baffle plates because, even though drag could not be reduced significantly, lessening lift and clockwise moment decreased the danger that the bridge might be washed out if struck by a tsunami.

ACKNOWLEDGEMENT
This study was supported by grants from Ritsumeikan University Research Projects on the Great East Japan Earthquake Disaster. Authors thank Mr. Wataru Itonaga, former graduate student of Ritsumeikan University, for his valuable help in the hydraulic experiments.

REFERENCES

Achmad, F., Fujima, K., Shigihara, Y. and Mizutani, N. (2009). Experimental study on tsunami forces: Estimation of tsunami force acting on structures related to run up distance, scale of building and pressure distribution. *Fifth International Conference on Asian and Pacific Coasts*. **Vol.1:** 114-121.

Kosa, K., Akiyoshi, S., Nii, S. and Kimura, K. (2011). Experimental study to evaluate the horizontal force to the bridge by tsunami. *Journal of Structural Engineering, JSCE*. **57A**, 442-453 (in Japanese).

Nakao, H., Izuno, K. and Kobayashi, H. (2009). Flow and hydrodynamic force characteristics associated with a tsunami acting on a bridge. *Journal of Structural Engineering, JSCE*. **55A**, 789-798 (in Japanese).

Nakao, H., Izuno, K. and Kobayashi, H. (2010). Study on relation of velocity and wave height to hydrodynamic force on bridges by tsunami. *Journal of Structural Engineering, JSCE*. **56A**, 564-575 (in Japanese).

Nakao, H., Itonaga, W., Matsuda, R., Izuno, K. and Kobayashi, H. (2011). Study on hydrodynamic force on bridge sections subjected to tsunami. *Journal of Japan Society of Civil Engineers, Ser. A2*, **67:2**, I-481-491 (in Japanese).

Nii, S., Kosa, K., Shoji, G. and Kimura, K. (2009). Experimental examination concerning tidal wave action power to bridge. *Journal of Structural Engineering, JSCE*. **55A**, 471-482 (in Japanese).

Shigihara, Y., Fujima, K. and Kosa, K. (2010). Reevaluation of tsunami force acted on the bridges of the neighborhood of Banda Aceh in the 2004 Indian Ocean tsunami. *Journal of Japan Society of Civil Engineers, Ser. B2*, **66:1**, 231-235 (in Japanese).

Shoji, G., Moriyama, T., Fujima, K., Shigihara, Y. and Kasahara, K. (2009). Experimental study associated with a breaking tsunami wave load acting onto a single span bridge deck. *Journal of Structural Engineering, JSCE*. **55A**, 460-470 (in Japanese).

Zhang, G., Usui, T. and Hoshikuma, J. (2010). Experimental study on a countermeasure for reducing tsunami wave force acting on superstructure of bridges. *Journal of Japan Society of Civil Engineers, Ser. A1*, **66:1**, 425-433 (in Japanese).